applied sciences

MDPI

Article

Research on Gearbox Fault Diagnosis Method Based on VMD and Optimized LSTM

Bang-Cheng Zhang [1,2], Shi-Qi Sun [1], Xiao-Jing Yin [1,*], Wei-Dong He [1] and Zhi Gao [1]

[1] School of Mechanical and Electrical Engineering, Changchun University of Technology, Changchun 130103, China; zhangbangcheng@ccut.edu.cn (B.-C.Z.); 18043027686@163.com (S.-Q.S.); 15289277044@163.com (W.-D.H.); gaozhi@ccut.edu.cn (Z.G.)

[2] School of Mechanical and Electrical Engineering, Changchun Institute of Technology, Changchun 130103, China

* Correspondence: yinxiaojing@ccut.edu.cn; Tel.: +86-181-4309-7876

Abstract: The reliability of gearboxes is extremely important for the normal operation of mechanical equipment. This paper proposes an optimized long short-term memory (LSTM) neural network fault diagnosis method. Additionally, a feature extraction method is employed, utilizing variational mode decomposition (VMD) and permutation entropy (PE). Firstly, the gear vibration signal is subjected to feature decomposition using VMD. Secondly, PE is calculated as a feature quantity output. Next, it is input into the improved LSTM fault diagnosis model, and the LSTM parameters are iteratively optimized using the chameleon search algorithm (CSA). Finally, the output of the fault diagnosis results is obtained. The experimental results show that the accuracy of the method exceeds 97.8%.

Keywords: fault diagnosis; variational mode decomposition; chameleon search algorithm; long short-term memory neural network; gearbox

check for updates

Citation: Zhang, B.-C.; Sun, S.-Q.; Yin, X.-J.; He, W.-D.; Gao, Z. Research on Gearbox Fault Diagnosis Method Based on VMD and Optimized LSTM. *Appl. Sci.* **2023**, *13*, 11637. https://doi.org/10.3390/app132111637

Academic Editors: Jose Machado and Douglas O'Shaughnessy

Received: 17 August 2023
Revised: 11 October 2023
Accepted: 17 October 2023
Published: 24 October 2023

1. Introduction

With the development of modern industry, gears have become one of the most critical parts of modern industry. Gearboxes have been widely used in various machines due to their fixed transmission ratio, high transmission torque, and compact structure. The gearbox has become a variable speed transmission component for all kinds of machines. According to Nippon Steel Corporation [1], gear failures account for about 10.3% of the total number of machine failures. According to the statistics regarding gearboxes' failure parts, the failure of the gear itself accounted for the largest proportion of failures, about 60%; the gear drive is an important part of induced machine failure. Therefore, gearbox fault diagnosis research has important significance.

Gearboxes are mechanical systems in which several components operate in a lubricated environment, and lubrication analysis, acoustic emission analysis, and vibration analysis can be applied to detect faults [2]. Among these, vibration signals have been widely considered. Many studies have proposed monitoring methods based on vibration signals. For example, S et al. proposed a comprehensive method for detecting and classifying rotating bearing faults in machines, by combining permutation entropy (PE) with Flexible Analytic Wavelet Transform (FAWT) methods. Healthy FAWT decomposition signals faulty bearing systems under different operating conditions. In decomposition, the PE value is used to calculate the signal and then it is provided as a feature vector for a support vector machine (SVM) classifier for different types and fault sizes [3]. The present paper provides a novel approach for a Network Intrusion Detection System using machine learning and deep learning. Our approach uses two MLP (Multi-Layer Perceptron) models, one with three layers and the other with six layers. Random Forest is also used for classification. These models are ensembled in such a way that the final accuracy is boosted and the testing time is reduced. The novelty of this paper lies in the choice and the combination of the models for network security [4]. Scholars have conducted in-depth research on the feature extraction and diagnosis methods of gearbox transmission faults based on vibration signals, and the current analysis methods based on the vibration signals of gearboxes mainly include Fourier transforms, empirical modal decomposition [5], ensemble empirical modal decomposition [6], wavelet packet decomposition [7], variational mode decomposition, and so on. These methods achieve, to some extent, the pre-processing of gearbox vibration signals and the classification and identification of transmission faults. Empirical modal decomposition can adaptively decompose vibration signals; however, the problem of modal aliasing is prominent, which makes the physical meaning of the missing decomposed modal components and the cause of the faults difficult to explain. Ensemble empirical modal decomposition is improved (based on empirical modal decomposition) by adding white noise signals, which suppresses the endpoint effect and modal aliasing to a certain extent, but its computational complexity increases. Wavelet packet decomposition solves the problem of insufficient extraction of high-frequency components of the signal based on a wavelet transform; however, its decomposition effect is very dependent on a manual wavelet base selection, which does not meet actual online diagnosis needs. Variational mode decomposition (VMD) solves the problem of modal aliasing, has a solid theoretical foundation, and can be used for better diagnosis.

VMD can better restore the original signal and adaptively decompose it into a time series with different frequencies that are relatively smooth. Therefore, in this paper, the vibration signal is analyzed by variational mode decomposition, to decompose the modal components that contain the information of normal and wear faults of gear transmission systems. In many cases, the VMD method provides a solid solution to the mode mixing problem in empirical mode decomposition (EMD) methods. As a result, this method has been used in many research areas such as mechanical diagnostics [8]. VMD methods have also provided good performance in planetary gearbox research, as was executed by Feng et al. using joint VMD-based amplitude and frequency demodulation analysis and by Yong Li et al. using VMD power spectral entropy and deep neural networks (DNNs) [9]. To detect faults in a two-stage planetary gearbox, Wu et al. demonstrated a new method based on Renyi entropy, two-dimensional VMD, full-vector spectral techniques, and compressive sensing [10]. To verify correctness, an experimental study of fault test signals from a gearbox was carried out [11]. Zhang et al. proposed a VMD based on the Locust Optimization algorithm for the selection of mode numbers and balance parameters [12]. These proposals provide a good solution for selecting the mode number [13].

Quantification of the fault information contained in a time series of vibration signals that have undergone variational mode decomposition can be calculated using time series complexity metrics, such as approximate entropy, arrangement entropy, and other methods. Among them, the permutation entropy (PE) method is based on the spatial characteristics of a time series. Based on the spatial characteristics of the time series, it amplifies the small changes in the signal, which is more effective than other indicators in the diagnosis of abnormal states of mechanical equipment. Therefore, this paper chooses to apply permutation entropy in the process of gear transmission feature extraction to reflect the dynamic changes in the time series in different states of transmission.

With the rapid development of computer technology in recent years, LSTM models based on deep learning theory [14] have been heavily researched in recent years. Compared with other data-driven models, the LSTM neural network shows better prediction results, but the model performance is still vulnerable to the influence of data series and initial values of model parameters. Its convergence performance is greatly reduced when the number of classifications increases due to the increase in sample size. For this reason, optimization algorithms can be introduced to optimize its parameters. Commonly used examples are grid search methods, genetic algorithm, etc., but these methods have large computational complexity and easily fall into local optimum and present other problems. For this reason, a new algorithm named intelligent optimization is introduced to perform parameter optimization and fault classification on LSTM models. There have been many studies on the analysis of runoff sequences and the optimization of model parameters' initial values [15]. For example, Sun constructed the idea of "decomposition–prediction–reconstruction" and used a variational mode decomposition LSTM neural network model for runoff prediction of the Three Gorges reservoir, and the results showed that the model could effectively improve the accuracy of runoff prediction [15]. Wei Qin et al. developed a simulated annealing long short-term memory network (SA-LSTM) model, which can more accurately describe the dynamic lag time relationship between hydropower stations [15]. However, most of these studies focus on single data series decomposition or initial value optimization of LSTM model parameters, while there are few research results combining both. In this paper, we propose a coupled model, including variational mode decomposition (VMD), chameleon search algorithm (CSA), and long short-term memory (LSTM) neural networks, which is used in the mechanical field for fault diagnosis of a gearbox.

On this basis, an optimization method for long- and short-sequence fault diagnosis of gearbox transmissions based on variational mode decomposition substitution entropy and the chameleon search algorithm is proposed, and the actual test data of a gearbox transmission are divided into a training set and a test set, and the training set and the test set are further divided into two sets each. The features of the training set are extracted using VMD-PE, and models in the test set are trained and fault-diagnosed using CSA–LSTM. The results show that the method can accurately and quickly identify gearbox faults under 60% to 110% rated pressure test conditions, which is better than existing methods.

The second part of this study describes the construction, inference, and optimization process of the gearbox fault diagnosis model based on the VMD algorithm and the improved LSTM algorithm. The third part describes the setup of the experimental platform and the relevant parameters and conducts experimental validation and comparative experiments on the method proposed in this paper through examples, which further verifies the superiority of the method. Fault classification and diagnosis are carried out by the improved long short-term memory neural network algorithm and the experimental results are analyzed. The fourth part is the summary of the whole paper and discusses the outlook for future work.

2. Feature Extraction of Vibration Signals Based on Variational Mode Decomposition and Arrangement Entropy

As depicted in Figure 1, the proposed model operates in a series of steps to assess the condition of a gearbox. Initially, vibration signals are captured from the gearbox at a motor speed of 1420 rpm, employing a sampling frequency of 10 kHz. These signals are recorded in various states of gear looseness and wear, as well as when the gearbox is in optimal condition. The second phase involves the implementation of VMD to dissect the vibration signals. For a gearbox in pristine condition, the VMD solely is adept at extracting pertinent data. However, when evaluating a gearbox with transmission defects, a combination of VMD and arrangement entropy proves instrumental in isolating the characteristic features of these imperfections. In the subsequent stage, the identification of patterns indicative of gear wear states is executed by the chameleon search-optimized long short-term memory sequence algorithm. This innovative approach is meticulously designed to delineate and recognize intricate patterns associated with various stages of gear deterioration. The final comparative analysis reveals the superior efficacy of the presented model over conventional methodologies. VMD outperforms empirical mode decomposition in signal decomposition efficiency. Similarly, arrangement entropy exhibits enhanced precision in quantifying fault features compared to multi-scale arrangement entropy and approximate entropy, among other time series complexity calculations. This rigorous assessment underscores the proposed model's enhanced accuracy and reliability in diagnosing and characterizing gearbox anomalies.

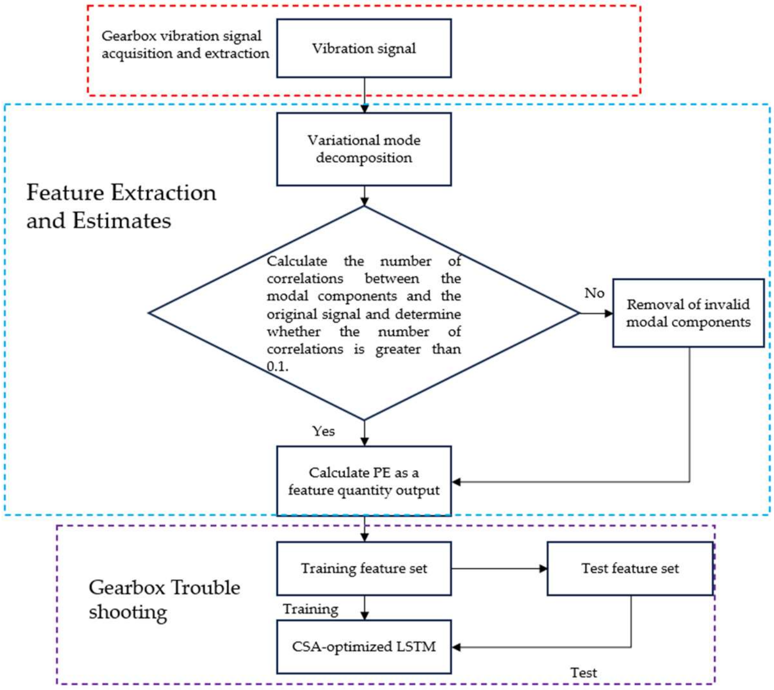

Figure 1. Overall flowchart of the proposed model.

2.1. Feature Extraction Methods

In this study, VMD and PE algorithms were employed to distill the fault characteristics inherent in the gearbox transmission. Figure 2 delineates the comprehensive flowchart outlining the intricate process of feature extraction, expounded in the subsequent steps. This systematic approach ensures a meticulous analysis, shedding light on the nuanced anomalies and operational inefficiencies within the gearbox transmission. The approach is outlined as follows:

(1) VMD decomposition of the vibration signal of the gearbox transmission is performed to obtain K components.
(2) The number of correlations between the original transmission vibration signal and the modal components decomposed by VMD is calculated. A value less than 0.1 indicates that it is a non-effective state component. A value less than 0.1 indicates that it is a non-valid state component, and the component is removed.
(3) The entropy of each modal component is calculated as a feature quantity.

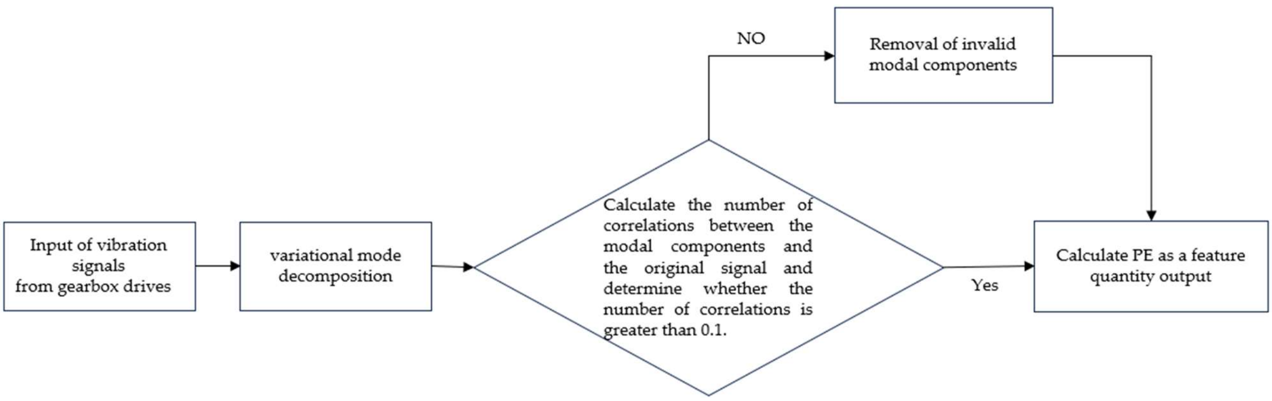

Figure 2. Flow chart of fault feature extraction.

2.2. Variational Mode Decomposition (VMD)

This article tackles the issue of limited robustness encountered during the extraction of fault feature frequencies within gearbox systems. Utilizing the VMD method, signals indicative of wear or tooth breakage faults within the gearbox are decomposed into several Intrinsic Mode Function (IMF) components. Subsequently, a correlation coefficient analysis is employed to meticulously identify those modal components that are imbued with fault signals. These selected components then undergo envelope spectrum analysis, a process that efficiently extracts and illuminates the fault feature frequencies, offering insights into the intricate dynamics of the gearbox's operational deficiencies. This refined approach enhances the precision and reliability of detecting and analyzing faults, thereby contributing to the optimization of maintenance and repair strategies.

Variational mode decomposition (VMD) is characterized as a fully non-recursive decomposition model. Introduced by Dragomiretskiy et al. in 2014, the essence of VMD is anchored in the utilization of central frequencies and bandwidths of the extracted modes [16]. The triumph of this decomposition technique is attributed to its approach of considering the solution as a constrained variational problem. Each process is meticulously crafted, ensuring that the extracted signals are both comprehensive and precise, thus bolstering the reliability and applicability of VMD in various analytical and diagnostic applications.

$$\underset{\{u_k\},\{o_k\}}{min}\{\sum_{k=1}^{K} \parallel \delta_t[(\delta(t)+\frac{j}{\pi t})\times u_k(t)]e^{-j\omega_k t} \parallel_2^2\} \tag{1}$$

$$subject\ to \sum_{k=1}^{k} u_k = f$$

where u_k denotes the decomposition mode, δ is the Dirac distribution, and $\times$ denotes the convolution. ω_k is the corresponding central frequency of the quadratic penalty term and Lagrange multipliers are introduced to solve the Equation (1). The augmented Lagrange quantities are shown below:

$$\begin{aligned} L(\{u_k\},\{\omega_k\},\lambda) = \alpha \sum_{k=1}^{k} \parallel \partial_t[(\delta(t)+\tfrac{j}{\pi t}) * u_k(t)]e^{-j\omega_k t} \parallel_2^2 \\ +Vf(t)-\sum_{k=1}^{K} u_k(t) \parallel_2^2 + \langle \lambda(t), f(t)-\sum_{k=1}^{K} u_k(t)\rangle \end{aligned} \tag{2}$$

where λ is the Lagrangian multiplier coefficient. The model number is provided in advance as a priori information K and the equilibrium reference α. Equation (2) can be solved by the alternating direction method of multipliers (ADMM) [17]. All decomposed modes and the corresponding central frequencies are then updated according to (3) and Equation (4), respectively:

$$\hat{u}_k^{n+1}(t) \leftarrow \frac{\hat{f}(\omega)-\sum_{i<k}\hat{u}_i^{n+1}(\omega)-\sum_{i>k}\hat{u}_i^{n}(\omega)+\frac{\hat{\lambda}^n(\omega)}{2}}{1+2\alpha(\omega-\omega_k^n)^2} \tag{3}$$

$$\omega_k^{n+1} \leftarrow \frac{\int_0^\infty \omega |\ \hat{u}_k^{n+1}(\omega)\ |^2 d\omega}{\int_0^\infty |\ \hat{u}_k^{n+1}(\omega)\ |^2 d\omega} \tag{4}$$

A detailed mathematical derivation and full algorithm for VMD can be found in [17]. VMD has been reported to have better performance in identifying fault features from noisy and complex vibration signals compared to local mean decomposition (LMD), ensemble empirical mode decomposition (EEMD), and conventional EMD [18].

2.3. Entropy of a Permutation (Physics)

Alignment entropy is a measure of the complexity of a time series that introduces the idea of alignment [19] and is commonly used for kinetic mutation detection as follows:

Let there be a time series $\{x_1, x_2, \cdots, x_N\}$ of length N for which the phase space reconstruction yields

$$X_i = \left\{x_i, x_{i+\tau}, \cdots, x_{i+(m-1)\tau}\right\} \tag{5}$$

In Equation (5): m is the embedding dimension; τ is the time delay. Ranking the quantities in X_i in ascending order, we have

$$x_{i+(j_1-1)\tau} \leqslant x_{i+(j_2-1)\tau} \leqslant \cdots \leqslant x_{i+(j_m-1)\tau} \tag{6}$$

In Equation (6), $j_1, j_2, \ldots, j_m$ are used to denote the column indexes where each element in X_i is located within the column index.

If two neighboring values are equal during the sorting process, they are sorted in ascending order by the subscript i of j_i. In this way, X_i is mapped to a set of symbols $S(k) = (j_1, j_2, \ldots, j_m)$, where $k = 1,2, \ldots, K$, where $K \leq m!$, embedded in the time series of dimension m; there are a total of $m!$ arrangements, that is, each m-dimensional subsequence X_i is mapped to one of $m!$ arrangements.

Calculate the probability of occurrence of each symbol sequence with $P_1, P_2, \ldots, P_K$, which is satisfied by

$$\sum_{k=1}^{K} P_k = 1 \tag{7}$$

Define the arrangement entropy of the time series $(x_1, x_2, \cdots, x_N)$ as

$$H(m) = -\sum_{k=1}^{K} P_k \ln P_k \tag{8}$$

The normal is ation of $H(m)$ is given as

$$H = H(m)/\ln m! \tag{9}$$

The value of H ranges from $0 \leq H \leq 1$. The smaller the value of H, the more regular the time sequence is and vice versa. The smaller the value of H, the more regular the sequence is and, vice versa, the more complex it is. The value of H amplifies the small and complex dynamics exhibited by the respective modal components of the normal and faulty states of the equipment.

2.4. Chameleon Search Algorithm (CSA)

The CSA is a novel meta-heuristic optimization algorithm based on the foraging strategy of chameleons proposed by Braik in 2021 [20]. This article optimizes the parameters of LSTM based on CSA. The algorithm focuses on solving the optimization problem through a three-stage position involving searching for prey, eye rotation to find prey, and capturing prey. The CSA is mathematically described as follows:

Initialization: The CSA begins by randomly initializing individuals of the chameleon population, each of which is a candidate solution to the target problem. Let the initial position of a chameleon individual with population size n in the dimensional search space be

$$x_{ij} = Ub + r \times (Ub - Lb) \tag{10}$$

where x_{ij} is the first i chameleon's j dimension and r is a random number uniformly generated in the range (0,1).

Searching for prey: Chameleon groups search for and find food during foraging primarily by location updating via Equation (6). The location update is mathematically described as

$$\begin{gathered} x_{ij}^{t+1} = x_{ij}^{t} + p_1 r_2 \left(P_{ij}^{t} - G_j\right) + p_2 r_1 \left(G_j - x_{ij}^{t}\right) \\ r \geqslant Pp \\ x_{ij}^{t+1} = x_{ij}^{t} + \mu[r_3(Ub - Lb) + Lb] sgn(rand - 0.5) \\ r < Pp \end{gathered} \tag{11}$$

where x_{ij}^{t+1} is the first ij-th dimensional space of a chameleon at the $t+1$ position of the second iteration. x_{ij}^{t} is the t-th iteration position in the j-th dimension of the chameleon and p_1 and p_2 are the development capacity control coefficients. r_1 and r_2 are random numbers uniformly generated in the range (0,1), P_{ij}^{t} is the position of the i t-th iteration of the j-th dimensional space of the chameleon at the best position, G_j is the iteration's globally optimal position of the chameleon, Pp is the chameleon perception probability, μ is the search ability control parameter, described as $\mu = e^{(-\alpha t/T)^*}$, α is the sensitivity coefficient, and T and t are the maximum and current iteration numbers.

The eyes rotate to spot prey. The chameleon's eyes can rotate 360° to search for prey and update their position based on the position of the prey. The position update is mathematically described as

$$x_i^{t+1} = m \times \left(x_i^t - \bar{x}_i^t\right) + \bar{x}_i^t \tag{12}$$

where x_i^{t+1} is the first i chameleon's $t+1$ position of the second iteration, x_i^t is the i-th iteration position of the chameleon, $\bar{x}_i^t$ is the position of the center of the iteration of the chameleon, and m is the rotation matrix.

Catching prey: When the prey is close to the chameleon, the chameleon uses its tongue to attack the prey and capture it. The position is updated mathematically, described as

$$x_{ij}^{t+1} = x_{ij}^t + \left[\left(v_{ij}^t\right)^2 - \left(v_{ij}^{t-1}\right)^2\right]/2a \tag{13}$$

where v_{ij}^t is the speed of the first i chameleon's current velocity, v_{ij}^{t-1} is the i velocity of the last iteration of the chameleon, a is the acceleration, and a = 2590 (1$-e^{-lgt}$).

2.5. Long Short-Term Memory (LSTM) Neural Network

The architecture of LSTM neural networks is intricately designed, comprising an input layer, a hidden layer, a recurrent layer, and an output layer. Addressing the challenges of gradient vanishing and explosion inherent in recurrent neural networks (RNN), LSTM neural networks incorporate memory unit states within the hidden layer. This modification fosters enhanced computational efficiency and learning precision. Within this hidden layer, control units are distinctly categorized into the input gate, forget gate, and output gate. The input gate is tasked with the selective recording of new information into the cell state, ensuring that only relevant data are assimilated. Conversely, the forget gate is instrumental in selectively discarding redundant or irrelevant information from the cell, optimizing the storage efficiency. The output gate then meticulously channels the retained information to the succeeding neuron. This selective retention and omission of information endow the LSTM neural network with the capacity for long-term memory, enabling it to adeptly extract temporal features. By meticulously curating and processing data, the LSTM neural network stands as a robust model for managing complex sequential and time series data, ensuring precision and reliability in predictions and analyses.

Initially, vibration signals indicative of gearbox faults were meticulously collected. Based on the distinct characteristics of these signals, an LSTM model was thoughtfully designed and calibrated. Subsequently, an illustrative analysis was undertaken wherein the original vibration signals, obtained from the gearbox, were decomposed utilizing the VMD method. This allowed for an intricate examination and processing of the signals, ensuring that nuanced features were not overlooked. The sorted dataset, enriched with comprehensive insights, was then subjected to temporal information fusion. This process was facilitated by the rigorously established long short-term memory neural network model, ensuring that the resultant data were both holistic and precise, ready for further analysis and interpretation.

$$f^{(t)} = \sigma\left(W_f h^{(t-1)} + W_f x^{(t)} + b_f\right) \tag{14}$$

where, σ is the Sigmid activation function. b_f is the threshold of the forgetting gate. W_f is the weight of the forgetting gate.

Update the two-part output of the input gate. The equation is

$$i^{(t)} = \sigma\left(W_i h^{(1-1)} + W_i x^{(1)} + b_i\right) \tag{15}$$

$$c'^{(t)} = \cdot\mathrm{anh}\left(W_c h^{(t-1)} + W_c x^{(t)} + b_c\right) \tag{16}$$

Update the cell state. The formula is

$$C^{(t)} = C^{(t-1)} * f^{(t)} + i^{(t)} * C'^{(t)} \tag{17}$$

where $C^{(t-1)}$ is the memory unit at moment $t-1$.

Update the output gate output. The formula is

$$o^{(t)} = \sigma\left(W_\circ h^{(t-1)} + W_\circ x^{(1)} + b_\circ\right) \tag{18}$$

$$h^{(t)} = o^{(t)} * \tanh\left(C^{(t)}\right) \tag{19}$$

where, $W_\circ$, $b_\circ$ are the weights and thresholds corresponding to the output gates, respectively. $h^{(t)}$ is the output vector of the hidden layer.

Update the forecast output at the current moment. The formula is

$$\tilde{y}^{(t)} = \sigma\left(Vh^{(t)} + c\right) \tag{20}$$

where V and c are the weights and thresholds of the implicit to-output layer connections, respectively. Equations (14)∼(20) comprise the process of LSTM forward propagation, and then the error between the predicted and actual values is back-calculated to update the weights and thresholds until the maximum number of iterations is satisfied.

2.6. Chameleon Search Algorithm for Optimizing Long Short-Term Memory Neural Networks

The classification efficacy of a long short-term memory neural network machine is contingent upon specific parameters. In pursuit of optimizing parameters c (penalty factor) and g (variance), we introduce the chameleon search optimization–long short-term memory neural network machine algorithm. This tailored approach is designed to meticulously refine these parameters, ensuring enhanced classification performance and accuracy in diverse applications. The specific steps of the chameleon search optimization–long short-term memory neural network algorithm are as follows:

(1) Import the training set and test set, and do the normal is action process;
(2) Initialize the parameters: initial penalty factor c_0, initial variance g_0, in the range of [21,22];
(3) Setting the eye rotation degree function, i.e., the function to be optimized, as the long and short-term neural network diagnostic accuracy function f with c and g as the relevant parameters, and adopting the chameleon search to find the optimum for c and g;
(4) When there is a situation where the eye rotation position is the same, i.e., the accuracy rate is the same, the combination of parameters with smaller value of c is selected to reduce the computational complexity;
(5) Iterate the loop until the maximum number of iterations N is reached;
(6) Output the position of the chameleon, i.e., the optimal values of c and g, which are used as the given parameters to train the long and short-term neural network model;
(7) Use the trained long and short-term sequence model to identify the gear wear level faults on the test set and derive the diagnostic results.

3. Comparison of Application Cases and Methods

This study employs a publicly accessible dataset for gearbox fault diagnosis, originally compiled by Zamanian, A.H., and colleagues in 2014, serving as a foundational resource for experimental validation [23]. The test rig underwent evaluations under varied pinion conditions, with vibration signals meticulously captured by accelerometers operating at a sampling rate of 10 kHz over a 10-second duration. The compiled data are organized into three distinct packages, each representing a specific fault type. These encompass datasets characterizing the healthy state, gear breakage, and gear wear conditions, providing a comprehensive spectrum for in-depth analysis and evaluation.

The core components of the test stand unit's drive system primarily include a motor that functions as the drive input. This motor propels the gearbox via a belt and, in turn, the gearbox's output drives the brake system, also connected by a belt. Data acquisition is facilitated by an accelerometer strategically positioned on the drive end of the induction motor [24]. With a sampling frequency set at 10 kHz and a sampling duration of 10 seconds, the parameters for data capture are meticulously defined. The motor operates at a speed of 1420 rpm/min. Given that the pinion gear is equipped with 15 teeth and the large gear with 110 teeth, the calculated meshing frequency equates to 355 Hz, derived from the formula $(1420/60) \times 15$. However, spectrum analysis reveals an actual meshing frequency proximate to 365 Hz, offering nuanced insights into the intricate dynamics of gear engagement and operation.

3.1. Comparison of Modal Decomposition Methods

To assess the efficacy of the integrated approach combining VMD alignment entropy and the CSA-optimized LSTM algorithm, a comprehensive validation was conducted, particularly focusing on performance under variational mode decomposition techniques. To meticulously evaluate the effectiveness of the combined VMD and CSA-optimized LSTM algorithm, experimental data were derived from the vibration signals of gearboxes in three distinct states: normal gearing, worn gears, and broken gears. These signals were analyzed under the stringent condition of 100% rated lubricating oil pressure to ensure an exhaustive examination of the algorithm's performance across a spectrum of operational and wear conditions, thereby underscoring its versatility and robustness.

The VMD algorithm initiates by pre-setting the number of decomposed modes, denoted as K. Illustratively, taking the vibration signal of a gearbox in its normal state, a Fourier transform is applied. This process yields a detailed spectrogram, vividly illustrating the vibrational signal characteristics of the gearbox in its pristine operational state. Following this, VMD decomposition is executed, effectively distilling the intrinsic vibrational modes and their respective characteristics.

The outcomes of this decomposition process are systematically illustrated in Figure 3, providing a visual and analytical insight into the vibrational dynamics of the gearbox. In this study, a random selection methodology was employed to curate the training set. Prior to initiating training, the original data from the gearbox underwent decomposition via VMD. Through iterative experimentation, it was observed that the VMD variational mode decomposition, when optimized using CSA, exhibited progressive convergence as the number of iterations increased. This methodological refinement ensures more accurate and consistent results, advancing our understanding of gearbox dynamics.

IMF_1 is a trend component that reflects the overall trend of gear speed changes in the gearbox dataset. IMF_2~IMF_n are the remaining random components, resulting in very small prediction errors.

When a transmission failure arises, alterations are observed not only in the fundamental frequency components but also in the octave components, each exhibiting varying degrees of suppression or enhancement. If the value of K is set at 3, the distinction between different models and the frequency components of the transmission vibration signal "a" becomes minimal. This makes the comprehensive extraction of fault-state information challenging. On the other hand, a K value exceeding 5 increases the complexity of the calculation significantly, introducing the risk of over-decomposition. Such a scenario is not optimal for prompt fault diagnosis due to the increased computational demands and potential for muddled insights. To strike a balance, we opted for a K value of 5. This allowed us to efficiently capture the center frequency of different modes inherent in the normal-state vibration signal of the gearbox transmission without compromising computational efficiency or clarity of insights. The time-domain plot derived from the VMD decomposition is depicted in Figure 3a, and the corresponding frequency spectrum is presented in Figure 3b, offering a visual and analytical exploration of the transmission dynamics.

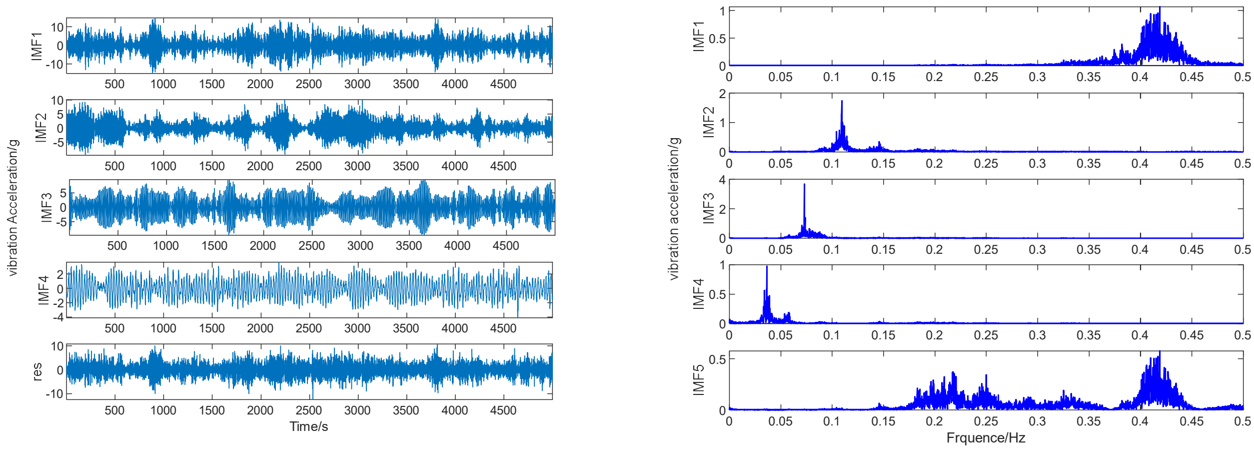

(**a**) (**b**)

Figure 3. Original data and VMD decomposition results of each sequence. (**a**) Time-domain diagram of the VMD decomposition. (**b**) Spectrogram of the VMD decomposition.

As can be seen in Figure 3, the modal aliasing phenomenon of VMD is effectively solved, and the corresponding center frequency of each modal component is consistent with the overall characteristics of the frequency derived from the fast Fourier transform, which realistically restores the information contained in the original signal. Compared with the existing empirical mode decomposition (EMD), the time-domain diagram of the transmission system's normal-state vibration signal decomposed by EMD is shown in Figure 4.

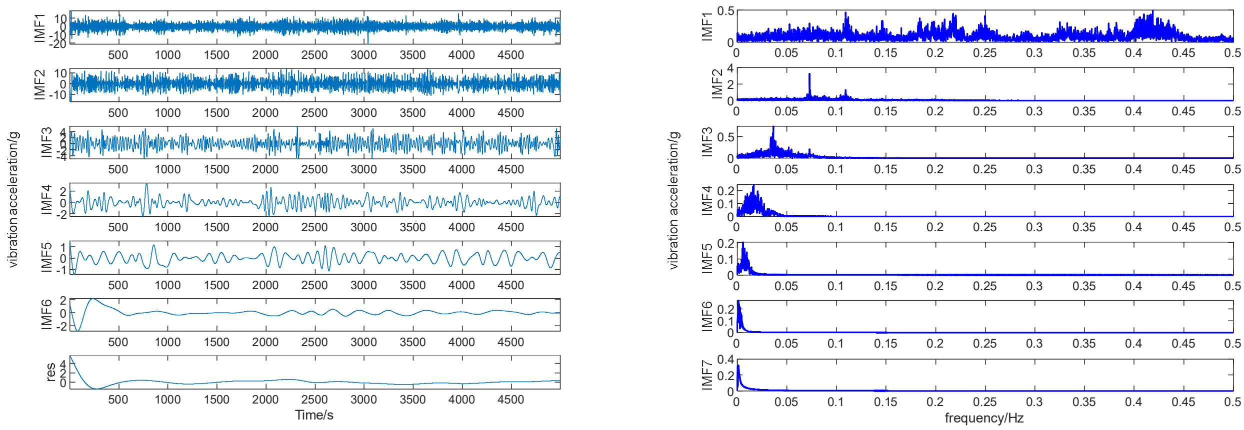

(**a**) (**b**)

Figure 4. Original data and EMD decomposition results of each sequence. (**a**) Time-domain diagram of the EMD decomposition. (**b**) Spectrogram of the EMD decomposition.

Figure 4 illustrates that as the quantity of decomposed modes escalates, overlapping of modes commences from mode 6 onward. This overlap gives rise to invalid components, which are ineffectual in representing information pertinent to the transmission's wear state. To mitigate the influence of these non-representative components, we introduced correlation number analysis. This technique calculates the correlation between each modal component and the chosen transmission vibration signal, ensuring that only valid and informative components are retained for subsequent analysis, enhancing the precision and reliability of the diagnostic insights.

The correlation between each modal component and the selected transmission vibration signal is calculated to distinguish valid from invalid components based on their ability to reflect the state of the transmission. Modal components with correlation coefficients exceeding 0.1 are deemed valid, as they effectively encapsulate the transmission-state information and are, therefore, selected for further analysis. Conversely, components with correlation coefficients below 0.1 are classified as invalid, lacking the capacity to serve as feature quantities indicative of the transmission's state. These low-correlation components are unable to accurately portray the variations in vibration signals distinguishing normal and fault conditions of the transmission and are consequently excluded from further consideration and analysis. This ensures that the subsequent evaluation and diagnostics are rooted in the most informative and representative data, enhancing the accuracy and reliability of the findings.

VMD-PE and EMD-PE are used to extract features from the vibration signals. m and τ are required to set the embedding dimension and delay time in advance for PE calculation, and $m = 6$ and $\tau = 1$ are generally chosen to better reflect the dynamics of the time sequence, so $m = 6$ and $\tau = 1$ are chosen. PE is calculated as the feature quantity of the modal components of the three states of transmission, with a total of 750 sets of data with 250 sets for each state of the transmission. We randomly select 200 sets of normal data, 200 sets of incomplete loosening data, and 200 sets of complete loosening data as the training set and the rest as the test set and carry out the training of the model and the classification of the results through the CSA-optimized LSTM algorithm. The diagnostic results are shown in Tables 1 and 2.

Table 1. VMD-PE fault diagnosis results.

Typology	Training Sample	Test Sample	Correct SAMPLE	Test Set Correctness/%
Healthy	200	50	50	100
Gear wear	200	50	50	100
Broken gear teeth	200	50	50	100
Aggregate	600	150	150	100

Table 2. EMD-PE fault diagnosis results.

Typology	Training Sample	Test Sample	Correct Sample	Test Set Correctness/%
Healthy	200	50	50	100
Gear wear	200	50	50	100
Broken gear teeth	200	50	47	94
Aggregate	600	150	145	96.67

Tables 1 and 2 clearly delineate the superior efficacy of the proposed method out- lined in this paper. It boasts a fault identification rate of 100% for diagnosing transmission wear associated with varying degrees of loosening. This impressive accuracy eclipses the 96.67% fault identification rate achieved by the EMD-PE method. This stark contrast in diagnostic precision attests to the robust capabilities of the VMD method in accurately discerning and isolating fault information related to gearbox transmission. The data underscore the method's exceptional performance, reinforcing its validity as a premier choice for intricate and reliable fault identification tasks.

3.2. Comparison of Time Series Complexity Metrics

The effectiveness of arrangement entropy in quantifying fault information for diagnosing gear-loosening faults during gearbox transmission is critically assessed. For a thorough evaluation, time series complexity indices including arrangement entropy, multi-scale arrangement entropy, approximate entropy, among others, are applied to the modal components decomposed by VMD.

The CSA-optimized LSTM algorithm is employed for fault diagnosis, facilitating an intricate analysis and classification of the data. This ensures that the assessment is both comprehensive and precise, illuminating the nuanced fault characteristics and their implications.

The diagnostic outcomes, which offer a detailed insight into the capability of arrangement entropy and comparable indices in capturing and quantifying fault information, are vividly displayed in Figure 5 and itemized in Table 3. This detailed presentation aids in the meticulous examination of the indices' performance, offering robust data to inform optimized fault diagnosis and maintenance strategies.

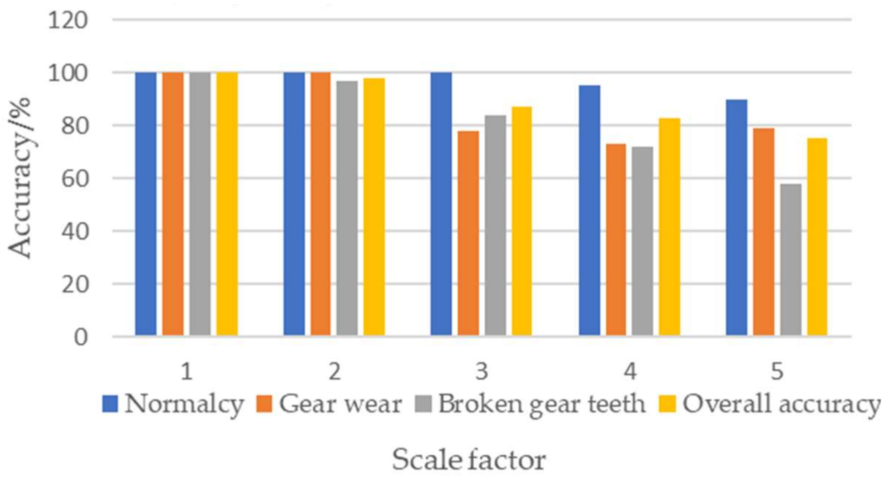

Figure 5. Permutation entropy of different scales.

Table 3. Complexity index of different time series.

Targets	Training Sample	Test Sample	Correct Sample	Test Set Correctness/%
entropy of disorder (physics)	600	150	150	100
Approximate entropy	600	150	143	95.3
Sample entropy (physics)	600	150	145	96.67
Fuzzy entropy (physics)	600	150	147	98

Insights gleaned from Figure 5 and Table 3 reveal a nuanced pattern in the performance of arrangement entropy in fault diagnosis. As the scale of arrangement entropy expands, there is a noted decline in the diagnostic accuracy for incomplete wear and broken gears. Despite this, arrangement entropy outperforms multi-scale arrangement entropy in quantifying fault information.

A comparative analysis with other indices underscores the superior efficacy of arrangement entropy, boasting a correct diagnosis rate that peaks at an impressive 100%. This remarkable precision is consistent, underscoring the robustness of arrangement entropy in capturing and articulating fault nuances.

These findings corroborate the assertion that arrangement entropy excels in dynamic detection performance during the diagnosis of loosening faults in gearbox transmission, outpacing other indicators. The metric's adeptness in encapsulating intricate fault dynamics underscores its pivotal role in enhancing the precision and reliability of diagnostic protocols in gearbox maintenance and repair.

3.3. Comparison of Optimization Algorithms

To assess the efficacy of the CSA-optimized LSTM model in diagnosing faulty gearbox transmissions, a comparative analysis was conducted deploying various optimization algorithms. These included the CSA-optimized LSTM algorithm and a grid search-optimized LSTM algorithm, among others, each applied systematically for fault diagnosis. Each algorithm's parameter settings are meticulously detailed in Table 4. The evaluation of these optimization algorithms' performance is anchored on two pivotal indices: the time required for computation and the correct diagnosis rate. These criteria offer a balanced perspective, encapsulating both the efficiency and accuracy dimensions of the algorithms' performance. The comparative outcomes, which provide a comprehensive insight into the relative performance and efficacy of each optimization algorithm, are tabulated in Table 5. These data serve as a robust foundation for evaluating the nuanced capabilities of the CSA-optimized LSTM model in the context of faulty gearbox transmission diagnosis, offering clear benchmarks for performance optimization and enhancement.

Table 4. Parameter setting of each optimization algorithm.

Optimization Algorithm	Parameter Is Action
CSA	The number of iterations is 200, and the initial c and g are random numbers from 1 to 5 in high
Grid Search	Initially c and g are random numbers from 1 to 5 with an initial step size of 0.1
Genetic algorithm	The number of iterations is 200 and the c and granges from 1 to 5
Particle swarm algorithm	The number of iterations is 200 and the c and granges from 1 to 5

Table 5. Performance comparison.

Optimization Algorithm	Computation Time/s	Test Set Correctness/%
CSA	3.87	100
Grid Search	9.12	99.4
Genetic algorithm	4.51	98.9
Particle swarm algorithm	15.23	100

As evidenced in Tables 4 and 5, the CSA optimization algorithm outperforms its counterparts, namely the genetic algorithm, grid search method, and particle swarm algorithm, in terms of convergence speed. Impressively, it attains a test accuracy of 100%, adeptly circumventing the common pitfall of overfitting. This underscores the CSA optimization algorithm's superior efficacy and optimization performance, marking it as a leading solution that combines speed, accuracy, and robustness in delivering optimal results.

3.4. Troubleshooting of Variable Pressure States

High-speed bearings and gear problems such as spalling, pitting, etc., are usually caused by insufficient local lubrication. Therefore, gear transmission and lubricant pressure are closely related.

Since the lubricant pressure is not always maintained at the rated pressure during the operation of a gearbox, to verify the effectiveness of the method in the fault diagnosis performance under variable pressure conditions, the method was developed and validated. The effectiveness of the method in fault diagnosis under variable pressure conditions is verified. We selected 20%, 40%, 60%, 80%, 100%, and 110% of the rated pressure of the gearbox transmission vibration data from 750 sets. Using the method proposed in this paper, gearbox transmission wear fault feature extraction and fault type identification were carried out. The diagnostic results are shown in Figure 6.

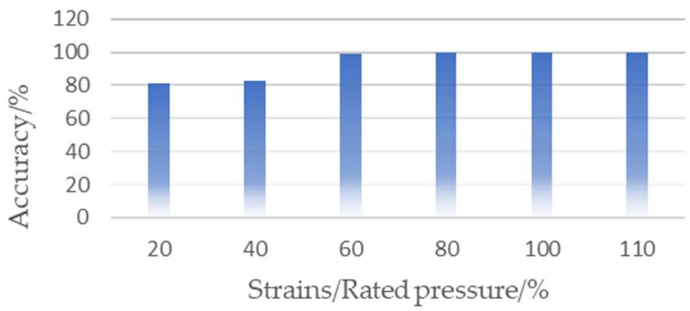

Figure 6. Fault diagnosis results under different pressure conditions.

As depicted in Figure 6, there is a marked increase in the correct diagnosis rate correlating with the rise in pressure, consistently peaking at 100%. In such scenarios, the vibration signals of the gearbox transmission are notably susceptible to various forms of interference, leading to the obscuring of essential fault-state information. However, a shift is observed with the augmentation of pressure. Distinctive vibration characteristics, emblematic of varied transmission states, are observed. During this phase, the pervasive influence of interference factors on the overall fault depiction is markedly subdued. This resilient performance amidst escalating pressures underscores the method's adeptness in meticulously extracting wear-related failure characteristics, attuned to the nuanced variations in lubricant pressure states of transmission. Such robust diagnostic precision reaffirms the method's validity, positioning it as a reliable asset in intricate fault detection and characterization.

3.5. Comparison of Different K Values for Troubleshooting

The choice of the K value plays a crucial role in effectively extracting information related to the state of gearbox transmission. It also significantly impacts the time taken for modal decomposition. The assertion that $K = 5$ is superior in fault diagnosis is examined in this context. To validate this claim, the K value is varied, and 750 sets of gearbox transmission vibration data are employed, all collected under a state of 100% rated pressure. The proposed method is then applied to extract characteristics indicative of wear faults in the gearbox transmission and to identify the specific types of faults present. The diagnostic outcomes, derived from this comprehensive analysis, are systematically presented in Table 6. This tabulation provides a detailed perspective on the efficacy of different K values in capturing and elucidating fault characteristics, offering valuable insights into the optimal K value for enhanced diagnostic accuracy and efficiency.

Table 6. Fault diagnosis results of different K values.

K-Value	Modal Decomposition Time/s	Test Set Correctness/%
4	2544	91.3
5	3486	100
6	6504	96.7

As illustrated in Table 6, a modal decomposition number of $K = 4$ proves to be inadequate, resulting in an insufficient extraction of transmission vibration information. This shortfall precipitates a nearly 10% decline in the diagnosis accuracy rate. Conversely, with $K = 5$, a balance is achieved; the modal decomposition is optimal, ensuring a moderate decomposition time and attaining a 100% correct diagnosis rate. When K is increased to 6, the decomposition time almost doubles compared to $K = 5$. This increase in modal decomposition time correlates with an over-decomposition scenario. The excess decomposition yields frequency components void of effective transmission-state information, leading to a nearly 10% reduction in the correct diagnosis rate. These findings corroborate that $K = 5$ is the optimal number for modal decomposition, striking a balance between efficiency and accuracy in extracting pertinent transmission vibration information, thereby ensuring diagnostic precision.

4. Conclusions

In this study, we focus on utilizing vibration signals to diagnose wear faults in gearbox transmissions. We introduce a novel diagnostic approach that integrates VMD-PE and CSA–LSTM to enhance the accuracy and efficiency of identifying such faults. The outcomes and insights derived from implementing this innovative method led us to the following conclusions:

(1) In this work, we present an optimized LSTM fault diagnosis method tailored for efficient and accurate transmission vibration signal diagnosis. The CSA is harnessed to meticulously iterate and optimize the LSTM parameters, enhancing the pattern recognition of gearbox wear faults. Through a comprehensive comparative analysis with existing optimization algorithms, our proposed method emerges superior in fault pattern recognition, computational time complexity, and diagnostic accuracy, affirming its robustness and efficacy in the intricate domain of fault diagnosis.

(2) This study introduces a feature extraction approach utilizing VMD and PE. This methodology enables adaptive mode decomposition of the transmission's vibration signals, facilitating the quantification of modes derived from the VMD-decomposed signal. By quantizing the state information encapsulated in the mod-al components of VMD decomposition, we effectively address the modal overlap issue associated with EMD. Our simulation test results for fault diagnosis under-score the efficacy of arrangement entropy in quantifying the state information embedded in the transmission component. Comparative analysis reveals that arrangement entropy outperforms multi-scale arrangement entropy, approximate entropy, and other time series complexity indicators in quantifying the transmission vibration signal, marking a significant advancement in the precision and reliability of fault diagnosis methodologies.

Author Contributions: Conceptualization, B.-C.Z., S.-Q.S., X.-J.Y., W.-D.H. and Z.G. All authors have read and agreed to the published version of the manuscript.

Funding: This work was supported in part by the Science and Technology Department of Jilin Province under Grant 20210201050GX, in part by the Major Science and Technology Projects of Jilin Province and Changchun City under Grant 20210301033GX.

Institutional Review Board Statement: Not applicable.

Informed Consent Statement: Not applicable.

Data Availability Statement: The data used in this article are inconvenient to declare.

Conflicts of Interest: The authors declare no conflict of interest.

References

1. Salameh, J.P.; Cauet, S.; Etien, E.; Sakout, A.; Rambault, L. Gearbox condition monitoring in wind turbines: A review. *Mech. Syst. Signal Process.* **2018**, *111*, 251–264. [CrossRef]

2. Wang, J.; Cheng, F.; Qiao, W.; Qu, L. Multiscale filtering reconstruction for wind turbine gearbox fault diagnosis under varying-speed and noisy conditions. *IEEE Trans. Ind. Electron.* **2017**, *65*, 4268–4278. [CrossRef]
3. Sharma, S.; Tiwar, S.K.; Singh, S. Integrated approach based on flexible analytical wavelet transform and permutation entropy for fault detection in rotary machines. *Measurement* **2021**, *169*, 108389. [CrossRef]
4. Sharma, S.; Tiwarl, S.K. A novel feature extraction method based on weighted multi-scale fluctuation based dispersion entropy and its application to the condition monitoring of rotary machines. *Mech. Syst. Signal Process.* **2022**, *171*, 108909. [CrossRef]
5. Zeng, X. *Research and Implementation of Condition Monitoring System for Power Transformer Based on Vibration Analysis*; South China University of Technology: Guangzhou, China, 2016.
6. Yu, X. *The Transformer Winding Deformation Detection System Based on Vibration Analysis*; Shanghai Jiao Tong University: Shanghai, China, 2016.
7. Zhang, B.; Xu, J.; Chen, J.; Li, H.; Lin, X.; Zang, Z. Diagnosis method of winding deformation based on power transformer vibration information. *High Volt. Eng.* **2015**, *41*, 2341–2349.
8. Li, Y.; Cheng, G.; Liu, C.; Chen, X. Study on planetary gear fault diagnosis based on variational mode decomposition and deep neural networks. *Measurement* **2018**, *130*, 94–104. [CrossRef]
9. Wu, Z.; Zhang, Q.; Cheng, L.; Tan, S. A New Method of Two-stage Planetary Gearbox Fault Detection Based on Multi-Sensor Information Fusion. *Appl. Sci.* **2019**, *9*, 5443. [CrossRef]
10. Kumar, A.; Gandhi, C.P.; Zhou, Y.; Kumar, R.; Xiang, J. Recent advances in the diagnosis and prognosis of gear defects: A review. *Measurement* **2020**, *158*, 107735. [CrossRef]
11. Zhang, X.; Miao, Q.; Zhang, H.; Wang, L. A parameter-adaptive VMD method based on grasshopper optimization algorithm to analyze vibration signals from rotating machinery. *Mech. Syst. Signal Process.* **2018**, *108*, 58–72. [CrossRef]
12. Isham, M.F.; Leong, M.S.; Lim, M.H.; Bin Ahmad, Z.A. Intelligent wind turbine gearbox diagnosis using VMDEA and ELM. *Wind Energy* **2019**, *22*, 813–833. [CrossRef]
13. Hu, Q.F. Preliminary study on LSTM model for daily runoff prediction at Ankang Station in Han jiang River Basin. *Adv. Geosci.* **2020**, *39*, 636–642.
14. Wang, S. Study of DFA_VMD_LSTM combined daily runoff prediction model. *Hydropower Energy Sci.* **2021**, *39*, 12–15.
15. Wei, Q. SA-LSTM-based dynamic hysteresis relationship of inter-station flow in hydropower plants. *Hydropower Energy Sci.* **2021**, *42*, 402–411.
16. Dragomiretskiy, K.; Zosso, D. Rational mode decomposition. *IEEE Trans. Signal Process.* **2014**, *62*, 531–544. [CrossRef]
17. Wang, Y.; Markert, R.; Xiang, J.; Zheng, W. Research on variational mode decomposition and its application in detecting rub-impact fault of the rotor system. *Mech. Syst. Signal Process.* **2015**, *60*, 243–251. [CrossRef]
18. Braik, M.S. Chameleon swarm algorithm: A bioinspired optimizer for solving engineering design problems. *Expert Syst. Appl.* **2021**, *174*, 114685. [CrossRef]
19. Bandt, C.; Pompe, B. Permutation entropy: A natural complexity measure for time series. *Phys. Rev. Lett.* **2002**, *88*, 174102. [CrossRef] [PubMed]
20. Zamanian, A.H. Experimental Dataset for Gear Fault Diagnosis. *Dataset Gear Fault Diagn.* **2014**. [CrossRef]
21. Tenbohlen, S.; Jagers, J.; Vahidi, F. Standardized survey of transformer reliability: On behalf of CIGRE WG A2.37. In Proceedings of the 2017 International Symposium on Electrical Insulating Materials (ISEIM), Toyohashi, Japan, 11–15 September 2017; pp. 593–596.
22. Zhang, F.; Ji, S.; Shi, Y.; Lu, W.; Li, D.; Chen, L. Research on transformer winding vibration and propagation characteristics. *Proc. CSEE* **2018**, *38*, 2790–2798.
23. He, F.; Ye, Q. A convolutional neural network based on wavelet packet transform and simulated annealing algorithm optimization for bearing fault diagnosis. *Sensors* **2022**, *22*, 1410. [CrossRef] [PubMed]
24. Montgomery, D.C. *Introduction to Statistical Quality Control*; John Wiley & Sons: New York, NY, USA, 2007; Volume 82, p. 398.